SELF-ASSEMBLED AGGREGATES OF NEUTRAL NONLINEAR OPTICAL DYES IN SMECTITE CLAY FILMS

By

Mark Kostuk

****

Submitted in partial fulfillment of the

requirements for Honors in the

Department of Chemistry

UNION COLLEGE

June 2001

ABSTRACT

KOSTUK, MARK Self-Assembled aggregates of neutral nonlinear optical dyes in smectite clay films. Department of Chemistry, June 2001.

The field of photonics relies on nonlinear optical (NLO) materials and their unique light interacting properties to guide and manipulate light for such uses as optical switches and optical data storage. Hybrid organic-inorganic composites offer excellent routes to such materials synthesis. We report herein the first study of neutral organic NLO chromophores adsorbed onto hectorite and laponite clay films. Seven different dyes (disperse red 1; disperse red 13; disperse red 19; disperse orange 3; disperse orange 13; disperse orange 25, and DANS, [4-dimethylamino-4'-nitrostilbene]), and two exchangeable cations (sodium and zinc), are used to create the hybrid films. The nature of the dye aggregation is characterized using UV/VIS spectroscopy, Xray diffraction, and second harmonic generation (SHG). Both J and H type aggregates are observed. The type and extent of aggregation is found to be primarily dependant on the functionalized structure of the dye molecule. The relative populations of aggregating versus bulk dye is found to depend on the amount of available clay surface area, which is affected by host clay particle size and the intergallery cation charge density. J aggregation is maximized at 0.10 w/w% dye in the zinc-laponite system. We found that the overall maximum dye loading levels are above 10 w/w% for the laponite system and between 1 and 5 w/w% for hectorite. Laponite is more ideally suited for optical device applications given its low background absorption. Currently the composite films do not show any second harmonic generation even though J aggregates have been shown to exhibit enhanced SHG in related systems.

ACKNOWLEDGEMENTS

Thank you Sam and Jason for laying the ground work for this project and for an enjoyable summer. Thank you Seyffie and Prof. McWhirter for your incredible help and knowledge in the laser lab. Thanks Mike for understanding what it means to be down to the wire.

I would like to thank our collaborators, The Apple Group at RPI and M. Eastman of NAU for your continued discussions and ideas. The insight and assistance you have provided has been invaluable. Without funding from the NSF-AIRE program, the Union College Summer Scholars program, or the Camille & Henry Dreyfus Foundation this project would not be have been possible.

TABLE OF CONTENTS

TABLE OF FIGURES

Introduction

Nonlinear optical (NLO) materials are important for the development of advanced photonic devices[1,2] such as optical switches for computers and holographic data storage media. These materials have the unique ability to manipulate light through effects such as second harmonic generation, wave-mixing, and the electro-optic effect[3]. One approach to the development of nonlinear optical materials[4] is through the fabrication of inorganic-organic hybrids.

Hybrid inorganic-organic composites comprise an amazing class of advanced materials with specifically tailored inner architecture leading to enhanced device capabilities.[5,6,24] The organic component offers a diverse selection of thermal, electrical and optical properties while the inorganic can serve to increase surface area, template and stabilize the guests. Control over the host structure, ordering and resultant environment affect the behavior of the guest and its desired interactions. Careful matching between the two components is essential for the creation of successful advanced materials.

Layered silicate clays are inorganic hosts that can be used to provide two-dimensional ordering, thermal, and temporal stability to a composite material. Hectorite is one such clay that is made of repeating tetrahedral-octahedral-tetrahedral layers (See Figure 1). Lithium cations doped onto magnesium inside the octahedral sites gives the clay layer an overall negative charge; in order to balance this negative charge, other cations (typically sodium) are incorporated into the intergallery region and bind adjacent layers together. These cations can be replaced through an exchange process allowing for different host characteristics in terms of redox potential, optical properties,[7,8] and film stability.

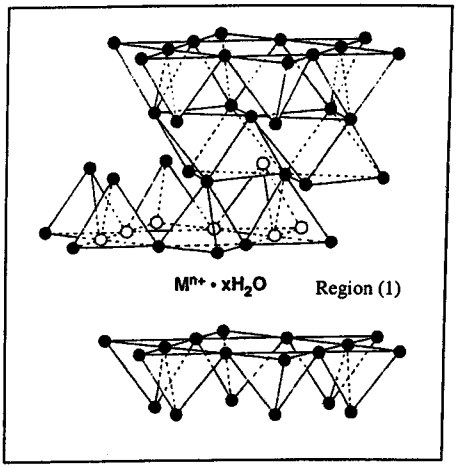

Figure 1. Intergallery region of a TOT layered clay such as hectorite or laponite.

Multiple TOT units and intergallery spaces stack on top of one another to form a microcrystallite, or tactoid, that in turn build like bricks to form macroscopic films. Laponite[9,10,11,12] is a synthetic form of hectorite with a similar chemical structure and TOT arrangement. It differs from hectorite in that the tactoid size of laponite is much smaller (300Å x 10Å)[13] and comprised of a *single* TOT unit. As a result of this smaller particle size, the laponite platelets have a very high edge charge and tend to form a gel-like matrix termed the 'house of cards' structure[14,3] where the platelets are both vertically as well as horizontally stacked as shown in Figure 2.

Clay films have three distinct regions that the organic guest molecules can reside in: (1) the intergallery region in between repeat TOT layers; (2) the surface of a clay tactoid; and (3) the micropore space between adjacent particles arising from defects in the layered

structure (See Figures 1& 2). The insertion of guest molecules into the intergallery region (1) of the clay is called intercalation. Differences in charge density, water content and the amount of clay contact affect the size and hydrophobicity of these microenvironments.

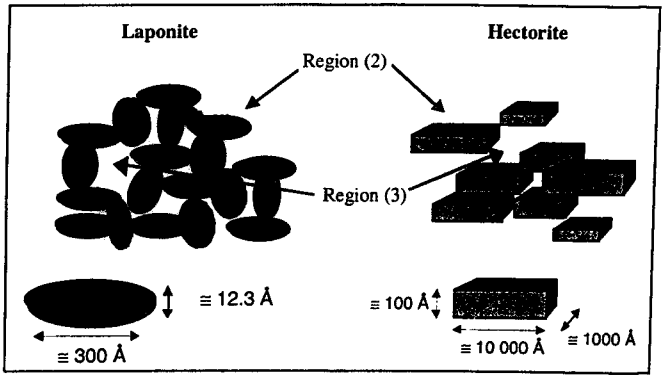

Figure 2. Difference in microcrystallite arrangement between laponite 'house of cards' structure and hectorite. Laponite tactoids are single TOT layers while a hectorite microcrystallite may contain seven to ten TOT layers.

The types of guest molecules that can be incorporated into the host are virtually limitless. Complex cations,[15,16] surfactants,[17,18,10] and positively charged dye molecules[19,17,7,20,21,22,23] have all been intercalated into similar systems. Combining charged nonlinear optical dyes into a clay host framework has shown much promise towards the development of materials with high nonlinearity.[24,25,7,26,22,23,27] The use of neutral organic dyes[28] allows for added hybrid variation and control through the choice of the intergallery cation. However it can be more difficult to obtain successful incorporation of the guest while avoiding phase separation between the organic and inorganic components.

The behavior of the dyes in the composites can be monitored through changes in electronic absorption spectra. The formation of different types of aggregates[19] is affected by the dye structure and the nature of its environment.[29] Sheibe or J-type aggregation[30,31,32,33] refers to the head-to-tail hydrogen bonding between neighboring dyes.

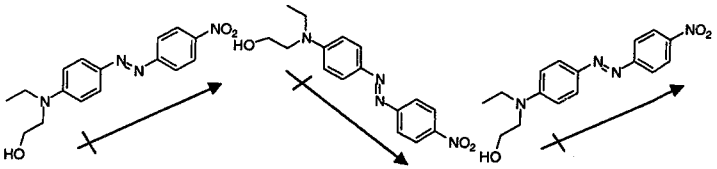

Figure 3. Head-to-tail hydrogen bonding of J aggregates.

J-Aggregation is evidenced by a red-shift in absorption spectrum as well as the presence of a new absorbance band that is typically associated with the formation of the dimer, or possibly higher aggregates. H-Type aggregation refers to π-stacking interactions between dye molecules, usually resulting in π-stacked dimerization.[30] The absorption spectra of H-aggregates show a characteristic single blue shifted peak.

The nature of the dye aggregation can have an affect on the photonic response of nonlinear optical materials. Certain dye arrangements often lead to NLO effects, while others do not. Second harmonic generation (SHG) is commonly used as a test for nonlinearity of these new composites. It occurs when incident light of frequency ω passes through a nonlinear medium that then emits light of twice the original frequency 2ω. SHG can be studied on powders,[34,35,36] colloidal suspensions,[14] and recently has been used to probe the noncentrosymmetric arrangement of dyes in films.[37,38,39,40,41,42,43,44]

The polarization equation below describes a materials interaction with applied electric fields. A nonlinear material is one that has large tensors that depend on higher order

terms of the electric field, such as $\chi^{(2)}$ (second order effects) or $\chi^{(3)}$ (third order effects). Throughout this work we are only concerned with second order nonlinearities ($\chi^{(2)}$).[3]

$$\mathbf{P} = \chi^{(1)}\mathbf{E} + \chi^{(2)}\mathbf{E}^2 + \chi^{(3)}\mathbf{E}^3 + \ldots$$

There are two main requirements for the specific production of materials with a high $\chi^{(2)}$ value; the first is the existence of permanent molecular electric dipoles. Conjugated organic molecules with electron donating-accepting functional groups[45,38,46,47,48,49,50,51,52,4] exhibit hyperpolarizability to applied electric fields. The second requirement for high $\chi^{(2)}$ materials is that these molecular dipoles are aligned in a noncentrosymmetric arrangement. If the dipoles are positioned such that they cancel there will be no NLO response. The host material can confer a high degree of spatial ordering to the organic guest molecules through layering, charge effects and influences on aggregation behavior.

In this work we report on novel hybrids of neutral NLO dye molecules incorporated into films of both hectorite and laponite clay host systems. UV/VIS absorption spectroscopy, X-ray diffraction and second harmonic generation studies are used to probe the clay structure and microenvironment of the guest in an effort to understand the influence of host ordering, guest concentration, and guest structure on dye aggregation and the resultant nonlinear optical response.

Experimental Section

The seven neutral dyes used for the synthesis of the hybrid materials were disperse red 1 (DSR1), disperse red 13 (DSR13), disperse red 19 (DSR19), disperse orange 3 (DSO3), disperse orange 13 (DSO13), disperse orange 25 (DSO25) and DANS, [4-

dimethylamino-4'-nitrostilbene]. All obtained from Aldrich & Co. and used as received. Refer to Figure 4 for the structure of these dyes. Two host clays were used: hectorite (hect), $Na_{0.66}[Li_{0.66}Mg_{5.34}Si_8O_{20}(OH)_4]$, (100 mmol/100 g cation exchange capacity (CEC))[53] from RHEOX Inc. and laponite (lap), $Na_{0.7}[Li_{0.3}Mg_{5.5}Si_8O_{20}(OH)_4]$, which has a similar composition, (72 mmol/100 g CEC) [11], from Southern Clay Products Inc.

Films are prepared with sodium or zinc as the intergallery cation of either clay host and with one of the seven dyes. The films will be referred to with their dye concentration, dye name and host clay; for example a 1% DSO3/ZnLap film contains 1% by weight disperse orange 3 adsorbed onto zinc exchanged laponite.

Since the clay comes prepared with sodium as the intergallery cation, films of sodium do not need to be exchanged. To create the sodium clay/dye mixture 400 mg of the clay and the desired weight percent of dye are ground together and suspended in 10 mL of water.

For the zinc cation exchanged films, 400 mg of the clay and the desired weight percent of dye are ground together and mixed in 100 mL 0.5 M $Zn(NO_3)_2$ for 48 hrs. The mixture is centrifuged and rinsed. The cleaned wet mixture is then re-suspended in 10 mL of water.

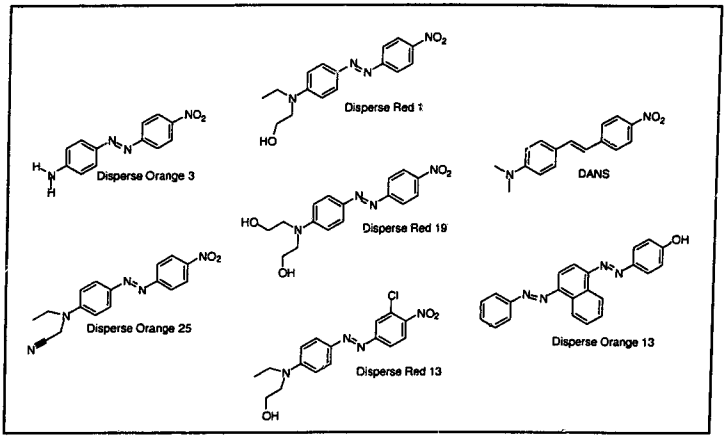

Figure 4. Structure of various NLO dyes used in this experiment.

To create films out of the suspensions they are thoroughly mixed for 48 hrs before being pipetted onto quartz microscope slides and allowed to dry slowly in a humidity controlled environment. The quartz slides are cleaned with acetone and dried prior to the casting of the films.

UV/VIS Spectra of all films were taken on a HP8453 spectrophotometer, and X-ray diffraction measurements were taken on a Philips PW1840 diffractometer using 1.788 Å Co K_α radiation. Second harmonic generation measurements were obtained using a Q-switched Nd:YAG laser (10 ns, 10 Hz, 1064 nm) and a photodiode spectrum analyzer. All experimental procedures and data collection were performed at room temperature.

Results and Discussion

Adsorption vs. Intercalation . Powder XRD spectra of clay films with and without dye do not show a significant difference in the d-spacing of the repeat unit indicating that the dyes are not intercalating into the intergallery region; region (1) (See Figure 1). Neutral guest molecules are not as readily intercalated as cationic species, however intercalation is not necessary for quality film formation. The use of neutral, hydrophobic dyes affords alternative strategies for composite assemblies through adsorption instead of intercalation.

The term 'adsorb' refers to the homogenous incorporation of a species within the framework of the clay host. Intercalation necessitates that such a species resides within the intergallery region (1), but an adsorbed material can be on the surface of a tactoid (2) or in the micropore space in-between adjacent tactoids (3) (See Figures 1 & 2).

When the clays are mixed with water they disperse into individual microcrystallites. In hectorite the space between multiple TOT layers swells with water which facilitates the ion exchange,[54] but with laponite the dispersed tactoids consist of only a single TOT layer; blurring the distinction between the surface and intergallery regions as well as making it difficult to talk about 'intercalation' as separate from adsorption.

When in solution, the hydrophobicity of the dye molecules drives it to aggregate with other dyes and to interact with the clay particles.[19,33] The clay-dye mixture is soluble as an aqueous suspension even though the dyes are all very insoluble in water. The UV/VIS spectra for the colloidal suspensions are identical to those of the films, thus indicating that the host and guest have begun interacting in the aqueous phase. Specifically the dye must be in contact with the surface of the clay tactoids and not simply trapped within micropore pockets as bulk phase dye because the micropore region is a product of film

formation and does not yet exist while in suspension. Whether the dyes are attached parallel or perpendicular to the surface normal of the clay is unclear, but a hydrophobic-entropic argument presumes that the dyes will try to minimize their exposed surface area to water and are therefore lying flat on the clay surface. The amount of clay surface area is therefore important for understanding the maximum possible amount of absorbed dye.

During the film formation process, the clay deposits on a substrate and the micropore space develops as gaps and defects arise due to tiling of the tactoids. At this point the laponite does have a tendancy to stack two or three TOT layers high in a parallel fashion,[14] creating a more formal intergallery space than what existed in solution.

The hectorite clay with sodium as the intergallery cation only forms powders and not stable films. The charge density of the alkali metal is not high enough to allow cohesion of the tactoid layers. If the sodium ion can coat the clay particle without residual positive charge to bind the next TOT microcrystallite the layering process stops.[33] Only with a higher charge cation, such as zinc, is the hectorite able to form films. The small size and increased edge charge of laponite allows it to form stable films even with sodium as a cation. This has profound implications for the use of these materials in photonic devices.

Comparison of Hectorite and Laponite. Figure 5 shows a comparison of UV/VIS spectra between a hybrid film of DSR1 made with hectorite and with laponite. One obvious difference is the background absorption of the two samples. The 1% DSR1/ZnLap film is much more optically transparent than the 1% hectorite film, allowing for the UV/VIS spectra of the dye to be much more resolvable from the clay matrix. This lower background is also important for the determination of the strength of

the nonlinear optical properties of the composite material and for the production of optical components in general.

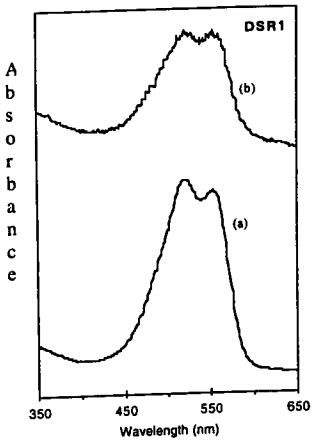

Figure 5. Comparison between films of 1% DSR1/ZnLap (a) and 1% DSR1/ZnHect (b). Laponite films show a much lower background absorbance.

The lower background absorption of the laponite is due to its smaller particle size and lack of scattering centers. Natural hectorite sequesters iron, a known optical scattering center, from the environment and incorporates it within the octahedral layers while the synthetic laponite is created in the absence of iron. The platelet size of the hectorite is around 1000 Å to 5000 Å[33] which is on the order of the wavelength of optical light causing serious scattering. The laponite platelet is much smaller, only about 300 Å[13], virtually eliminating this scattering effect.

As a consequence of the house-of-cards stacking, laponite films are not as lamellar as the hectorite films. This can be clearly seen in Figure 6, an X-ray comparison of the (00*l*) reflections of a laponite and hectorite film.

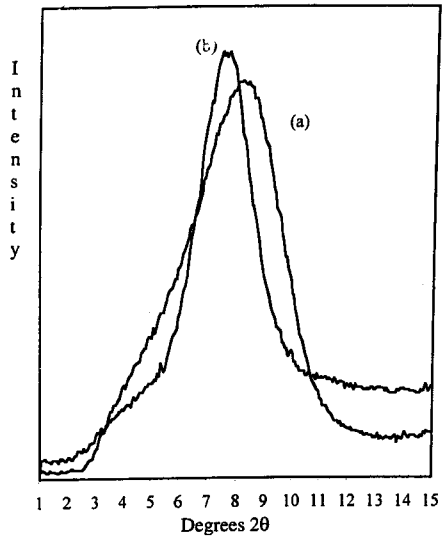

Figure 6. XRD spectra Laponite (a) and Hectorite (b) films.

The large FWHM of the laponite XRD pattern, with a basal spacing of 12.4 Å , indicates the existence of a range in the sizes of diffracting planes and a smaller crystallite size. While the hectorite pattern shows a narrower distribution centered at 13.5 Å, owing to the more consistent layering of TOT layers within a single microcrystallite.

UV/VIS of Clay/Dye Films. There are two important differences in the UV/VIS spectra of the hybrid films containing DSR1, DSR13, DSR19, and DSO25 as compared to the spectra of the bulk dye in acetone solution. The first is that the peak absorbance of these dyes is shifted to the red by 50 to 100 nm when in the composite material relative to solution. The second is the that the shape of the absorption spectrum of the composite material shows multiple bands compared to the simple Gaussian peak of the bulk dye.

The shape and red shift of the absorption spectra of DSR1, DSR13, DSR19, and DSO25 in Figure 7 are very characteristic of molecules undergoing J type aggregation[30]. The extended nature of the J aggregated dyes lowers the energy of excitation resulting in a red shift. The extent of red shift is related to the strength of the hydrogen bonding interactions. The presence of a chlorine ortho to the nitro group in DSR13 pulls electron density from the hydrogen bonding oxygen and reduces the strength of the hydrogen bond. This results in a red shift for the DSR13 composite of only 25 nm instead of 100 nm observed in the spectra of DSR1 and others.

The absence of a hydrogen donor on DANS does not allow it to hydrogen bond with itself; eliminating the possibility for J aggregation to occur. Instead the majority of this dye exhibits a blue shifted absorbance peak, evidence of H type aggregation (see Figure 8). The DANS spectrum *does* in fact show a slight peak akin to the J aggregation peaks observed above which can be attributed to hydrogen bonding through water.

The spectrum of disperse orange 3 exhibits an unusual plateau feature that is most likely due to the presence of a third band located between the two that are observed for the majority of the other hydrogen bonding dyes.

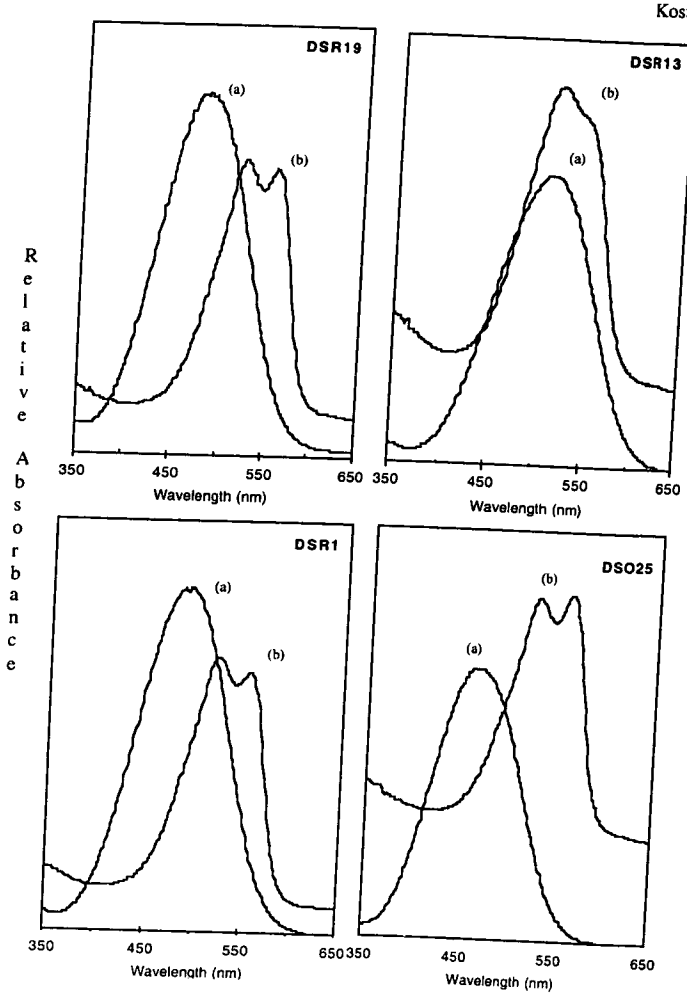

Figure 7. UV/VIS Spectra of DSR1, DSR13,DSR19, and DSO25 in acetone (a) and in a 1% Zn laponite film (b).

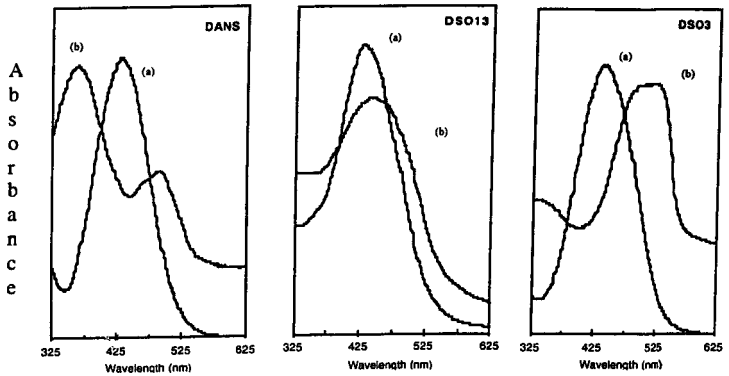

Figure 8. UV/VIS Spectra of DANS, DSO13 and DSO3 in acetone (a) and in a 1% Zn laponite* film (b). *The spectrum of DSO13 in Figure 8 is of a sodium laponite film, not a zinc film

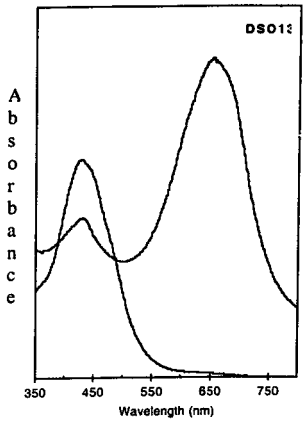

Figure 9. UV/VIS spectrum of DSO13 in acetone(a) and in a 1% Zn/Lap film (b). The dye is nitrated by the NO_3^- counter anion to produce a 200 nm redshifted absorption peak.

Disperse orange 13 has a much different structure than the other dyes and does not appear to be aggregating in either way. Stable, homogeneous films of DSO13 are still created even without any apparent aggregation. *It must be stated that the spectrum of DSO13 in Figure 8 is of a sodium laponite film, not a zinc film. It is hypothesized that the catalytically active clay nitrates the DSO13 dye using the NO_3^- counter anion of the zinc solution, resulting in a 200nm red-shifted absorption spectrum (see Figure 9). The details of this are not pursued further in this paper.

Effects of Dye Concentration. In Figure 10 the absorption spectra of DSR1 in low concentrations (0.01%, (b)) exhibits the characteristic J aggregation peak indicating its interactions with the clay surface and other dye molecules. As the concentration increases the environment sampled by the dye becomes more organophilic; likewise the absorption spectra shows that a larger population exists as bulk dye compared to the population J aggregating. It takes a higher concentration of chromophore before the dye exhibits bulk phase character in zinc laponite compared to sodium laponite.

A qualitative measure of the relative populations of dye in the composite films can be obtained if we ratio the intensities at 540nm, the red-shifted aggregation peak, to 490nm, the bulk dye absorption peak. Figure 11 shows that the dye in sodium laponite films reaches a maximum ratio of aggregated dye versus bulk dye at a concentration below 0.1% and drops sharply whereas the zinc laponite films contain a higher fraction at all concentrations. The zinc laponite film has an appreciable fraction of aggregated chromophore as high as 5%.

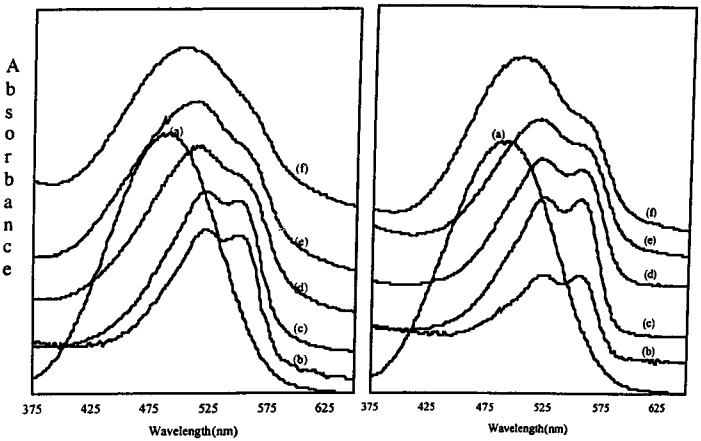

Figure 10. Absorption spectra with DSR1 (a) as a comparison between sodium laponite (left) and zinc laponite (right) loaded at 0.01% (b), 0.1% (c), 1% (d), 5% (e), and 10% (f). Note that the zinc films retain the J-aggregate peak structure at higher dye concentrations than the sodium films.

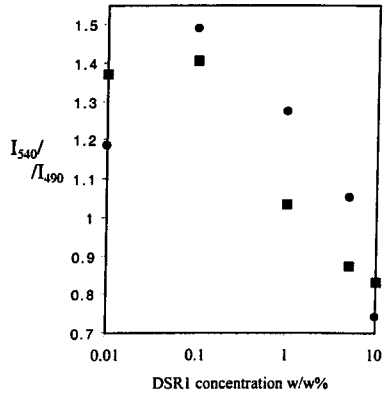

Figure 11. Relative intensities of the aggregated dye (540nm) to the bulk dye peak (490nm) for NaLap (■) and ZnLap (●). The NaLap reaches a maximum level of aggregated dye before 0.1% whereas the ZnLap maintains a much higher relative amount through 5%.

The analogous spectrum of dye loaded hectorite is impossible to create owing to the clay's high absorbance background. However we can still make some determinations about its maximum sustainable dye loading levels.

Figure 12 clearly show the loss of hectorite crystallinity as a function of dye concentration. At low dye concentration (0.01% by wt., (a)) the (001) peak of the hectorite at 12.6 Å is very sharp, as the concentration is increased the crystallinity decreases owing to an initial disruption of the platelet stacking. As the concentration is increased between 0.1% and 1% the crystallinity remains constant as the surface of the platelets is filled with dye. At concentrations above 1% dye the clay peak disappears as the dye occupies a significant portion of the film, hindering the layered structure. Figure 13 is a schematic depicting this disruption of tactoid stacking that occurs with increased dye loading.

The hectorite forms powders instead of films at concentrations of 5 and 10 w/w% dye indicating that the maximum hectorite loading level is between 1% and 5% dye; the maximum loading level for laponite is between 10% and 15%. As the concentration approaches these levels, control over the humidity and rate of evaporation becomes very important for the formation of quality films.

The larger crystallite size and flat layering of the hectorite means that it packs more densely than the 'porous' laponite when forming films. The house-of-cards structure of the laponite provides more available clay surface area for the dye to bind too. This available space for dye dictates the maximum allowable loading level before phase separation, which is much lower for the hectorite system than the laponite system. The higher charged cation (Zn^{+2} vs. Na^{+}) allows the laponite to flocculate more and encourages the edge-surface

interactions that lead to more expression of the house-of-cards formation.[33,14] The increased aggregated dye fraction for zinc laponite shows that the clay surface plays an integral role in determining the amount of dye aggregation.

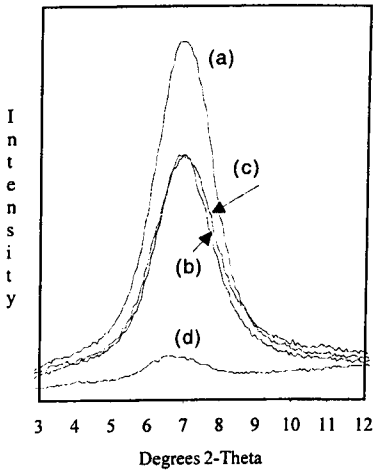

Figure 12. XRD data showing loss of crystallinity of DSR1/ZnHect films as dye concentration is increased from 0.01% (a), to 0.1% (b), 1% (c), and 10% (d).

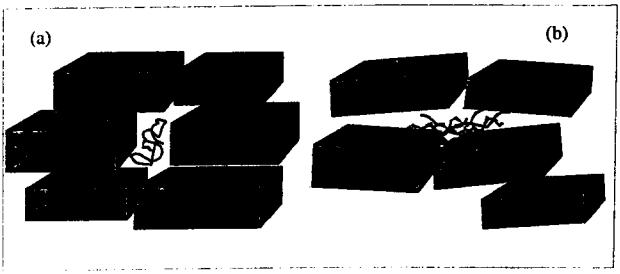

Figure 13. Schematic showing the loss of crystallinity due to increased amounts of dye in region 3. Low amounts (a) and higher amounts (b).

Nonlinear Optical Properties. Second harmonic generation was used to probe the nonlinear characteristics of the hybrid films. The polarized Nd:YAG fundamental of 1064 nm was incident upon the sample mounted on a rotating platform. The fiber optic spectrum analyzer is directly interfaced with a computer that is then used to determine whether second harmonic (532 nm) light is emitted. The generation of second harmonic light is strongly angle dependent and should approach its peak at a glancing angle of 90° to the film normal. The sample was rotated throughout all angles, 0-90° with respect to the film normal, but no measurable second harmonic light was observed. The detector was arranged to test for SHG in both reflection[37,38] and transmission.

A possible explanation for the lack of observed signal is that we are working outside of the peak dye concentration range for SHG, either with too high a dye concentration or too thick of a film. At very low dye concentration, there is not enough NLO material to create second harmonic light. With too high a concentration the NCS arrangement of molecules can be lost. The combination of these effects results in the existence of a critical dye level for SHG. The dye level for maximum SHG response of a material is not necessarily correlated to the maximum dye loading levels of the host, or to the peak aggregated dye fraction.

For nonlinear optical effects, J type aggregation is generally favored and H type aggregation is not.[7,8] The π-stacking typically results in a cancellation of molecular dipoles, destroying the possibility for a net electric field throughout the material. J-Type aggregation encourages a head-to-tail arrangement of dye molecules that leads to a non-centrosymmetric arrangement of dipoles resulting in higher χ^2 values for the composite.

The dyes used all have strong absorption in the second harmonic region (532nm). This also has competing effects on the NLO response. As a result, the molecules are easily excited electronically which creates a strong SHG response. Unfortunately at high dye concentration the SHG produced will not escape the material before being absorbed by other dye molecules. Maximizing the relative loading level for aggregated versus bulk populations is an important step in the creation of thin NLO composites. The aggregated dye has a higher possibility for emission of SHG[7,8] rather than absorption because of its NCS arrangement, whereas the bulk dye exhibits the opposite effect.

Conclusions

We have successfully created new hybrid inorganic-organic composites using neutral NLO dye molecules with both hectorite and laponite clays. The neutral dyes do not intercalate into the intergallery region of the clay. Through observations of the relative intensities of the aggregated and bulk dye spectra, we have determined that both sodium and zinc laponite have a peak aggregated dye fraction at around 0.1% dye by weight. The hectorite fraction is undeterminable due to a high background absorption by the host framework. Zinc laponite's aggregated fraction is at a slightly higher concentration than sodium laponite's, and maintains a significantly higher aggregated fraction at dye concentrations as high as 5% by weight.

The maximal loading limit of neutral dyes for zinc hectorite is found to be between 1% and 5% by weight, while for laponite it is between 10% and 15%. Sodium hectorite does not form stable films. The differences in loading limits and aggregated fraction are attributed to the exposed clay surface area to the dye. Exposed surface area is dependant on the charge density of the intergallery cation through effects on the extent of

clay tactoid flocculation. The smaller laponite particles have a higher tendency to flocculate and form the house-of-cards structure, resulting in the existence of more surface area for dye aggregation.

The lack of second harmonic generation imply that we do not have a non-centrosymmetric arrangement of chromophores, or that we are working outside of the peak SHG dye concentration. J aggregates have been shown to exhibit a strong SHG response and it is our belief that future work will locate the maximal dye concentrations needed for observable second harmonic generation.

References

[1] Bennion, I. *Inst. Phys. Conf. Ser. No 103: Introduction.* **1989.**

[2] Seto, J.; Tamura, S.; Asai, N.; Kishii, N.; Kijina, Y.; Matsuzawa, N. *Pure & Appl. Chem.* **1996**, 68(7), 1429-1434.

[3] Saleh, B. E. A.; Teich, M. C. *Fundamentals of Photonics* **1991**, John Wiley & Sons Inc. NY.

[4] Marder, S. R.; Sohn, J. E.; Stucky, G. D. *ACS Symposium Series 455*, **1991**.

[5] Bennion, I. *Inst. Phys. Conf. Ser. No 103: Introduction.* **1989.**

[6] Seto, J.; Tamura, S.; Asai, N.; Kishii, N.; Kijina, Y.; Matsuzawa, N. *Pure & Appl. Chem.* **1996**, 68(7), 1429-1434.

[7] Coradin, T.; Clément, R. *Chem. Mater.* **1996**, 8, 2153-2158.

[8] Lacroix, P. G.; Veret Lemarinier, A. V.; Clément, R.; Nakatani, K.; Delaire, J. A. *J. Mater. Chem.* **1994**, 3(5), 499-503.

[9] Mourchid, A.; Delville, A.; Lambard, J.; Lécolier, E.; Levitz, P. *Langmuir* **1995**, 11, 1942-1950.

[10] Brahimi, B.; Labbe, P.; Reverdy, G. Langmuir 1992, 8, 1908-1918.

[11] Saunders, J. M.; Goodwin, J. W.; Richardson, R. M.; Vincent, B. *J. Phys. Chem. B* **1999**, 103, 9211-9218.

[12] Bonn, D.; Kellay, H.; Tanaka, H.; Wegdam, G.; Meunier, J. *Langmuir* **1999**, 15, 7534-7538.

[13] Laponite Technical Directory, Laporte Ltd.

[14] Yan, E. C. Y.; Eisenthal, K. B. *J. Phys. Chem. B* **1999**, 103, 6056-6060.

[15] Tamura, K.; Setsuda, H.; Taniguchi, M.; Yamagishi, A. *Langmuir* **1999**, 15, 6915-6920.

[16] Liu, Z.; Ooi, K.; Kanoh, H.; Tang, W.; Yang, X.; Tomida, T. *Chem. Mater.* **2001**, 15, 475-478.

[17] Sonobe, K.; Kikuta, K.; Takagi, K. *Chem. Mater.* **1999**, 11, 1089-1093.

[18] Basini, L.; Raffaelli, A. *Chem. Mater.* **1990**, 679-684.

[19] Gessner, F.; Schmitt, C. C.; Neumann, M. G. *Langmuir* **1994**, *10*, 3749-3753.

[20] Coradin, T.; Nakatani, K.; Ledoux, I.; Zyss, J.; Clément, R. *J. Mater. Chem.* **1997**, 7(6), 853-854.

[21] Chaudhuri, R.; López Arbeloa, F.; López Arbeloa, I. *Langmuir*, **2000**, 16, 1285-1291.

[22] Lacroix, P. G.; Clément, R.; Nakatani, K.; Zyss, J.; Ledoux, I. *Science* **1994**, Vol. 263, 658-660.

[23] Ogawa, M. *Chem. Mater.* **1996**, 8(7), 1347-1349.

[24] Ogawa, M.; Kuroda, K. *Chem. Rev.* **1995**, 95, 399-438.

[25] Ogawa, M.; Takahashi, M.; Kuroda, K. *Chem. Mater.* **1994**, 6(6), 715-717.

[26] van Duffel, B.; Verbiest, T.; Van Elshocht, S.; Persoons, A.; De Schryver, F. C.; Schoonheydt, R. A. *Langmuir* **2001**, 17, 1245-1249.

[27] Lebeau, B.; Brasselet, S.; Zyss, J.; Sanchez, C. *Chem. Mater.* **1997**, 9, 1012-1020.

[28] Endo, T.; Nakada, N.; Sato, T.; Shimada, M. *J. Phys. Chem. Solids* **1988**, 49(12), 1423-1428.

[29] Liu, X.; Thomas, J. K. *Langmuir* **1991**, 7, 2808-2816.

[30] Möbius, D. *Adv. Mater.* **1995**, 7, No. 5, 437-444.

[31] von Berlepsch, H.; Böttcher, C.; Dähne, L. *J. Phys. Chem. B* **2000**, 104, 8792-8799.

[32] Friedrich, J.; Schneider, S. *Adv. Mater.* **1995**, 7(5), 435-436.

[33] López Arbeloa, F.; Hérrán Martínez, J. M.; López Arbeloa, T.; López Arbeloa, I. *Langmuir* **1998**, 14, 4566-4573.

[34] Kurtz, S. K.; Perry, T. T. *J. Appl. Phys.* **1968**, 39(8), 3798-3813.

[35] Dougherty, J. P.; Kurtz, S. K. *J. Appl. Cryst.* **1976**, 9, 145-158.

[36] Kiguchi, M.; Kato, M.; Kumegawa, N.; Taniguchi, Y. *J. Appl. Phys.* **1994**, 75(9), 4332-4339.

[37] Kim, H. K.; Kang, S.; Choi, S.; Min, Y.; Yoon, C. *Chem. Mater.* **1999**, 11, 779-788.

[38] Li, F.; Jin, L.; Huang, C.; Zheng, J.; Gui, J.; Zhao, X.; Liu, T. *Chem. Mater.* **2001**, 13, 192-196.

[39] Shimazaki, Y.; Ito, S. *Langmuir* **2000**, 16, 9478-9482.

[40] Liu, Y.; Hu, W.; Xu, Y.; Liu, S.; Zhu, D. *J. Phys. Chem. B* **2000**, 104, 11859-11863.

[41] Yam, V. W.; Yang, Y.; Yang, H.; Cheung, K. *Organometallics* **1999**, 18, 5252-5258.

[42] Ashwell, G. J.; Walker, T. W.; Leeson, P. *Langmuir* **1998**, 14, 1525-1527.

[43] Koetse, M.; Laschewsky, A.; Mayer, B.; Rolland, O.; Wischerhoff, E. *Macromolecules* **1998**, 9316-9327.

[44] Yam, V.; Wang, K.; Wang, C.; Yang, Y.; Cheung, K. *Organometallics* **1998**, 17, 2440-2446.

[45] Prasad, P. N.; Reinhardt, B. A. *Chem. Mater.* **1990**, 2, 660-669.

[46] Meyers, F.; Brédas, J. L. *International Journal of Quantum Chemistry* **1992**, 42, 1595-1614.

[47] Kaino, T.; Tomaru, S. *Adv. Mater.* **1993**, 5(3), 172-178.

[48] Marder, S. R.; Perry, J. W. *Adv. Mater.* **1993**, 5(11),804-815.

[49] Groenedaal, L.; Bruining, M. J.; Hendrickx, E. H. J.; Persoons, A.; Vekemans, J. A. J. M.; Havinga, E. E.; Meijer, E. W. *Chem. Mater.* **1998**, 10, 226-234.

[50] Dalton, L. R.; Harper, A. W.; Ghosn, R.; Steier, W. H.; Ziari, M.; Fetterman, H.; Shi, Y.; Mustacich, R. V.; Jen, A. K.-Y.; Shea, K. J. *Chem. Mater.* **1995**, 7, 1060-1081.

[51] Marder, S. R.; Perry, J. W.; Yakymyshyn, C. P. *Chem. Mater.* **1994**, 6, 1137- 1147.

[52] de la Torre, G.; Vázquez, P.; Agulló-López, F.; Torres, T. *J. Mater. Chem.* **1998**, 8(8), 1671-1683.

[53] Eastman, M. P.; Bain, E.; Porter, T. L.; Manygoats, K.; Whitehorse, R.; Parnell, R. A.; Hagerman, M. E. *Appl. Clay Sci.* **1999**, 15, 173-185.

[54] Annabi-Bergaya, F.; Estrade-Szwarckopf, H.; Van Damme, H. *J. Phys. Chem.* **1996**, 100, 4120-4126.